Pure & Appl. Chem., Vol. 61, No. 6, pp. 1075–1084, 1989.
Printed in Great Britain.

Heat capacity and structure in strongly-interacting systems

Lina Andreoli-Ball, Miguel Costas, Pierre Paquet, Donald Patterson* and Marie-Esther St. Victor

McGill University, Department of Chemistry, 801 Sherbrooke St. W., Montreal, PQ, Canada H3A 2K6

Abstract - The heat capacity has been used to reveal H-bonded multimers, predominantly tetramers, in solutions of 1-alkanols in inert solvents, e.g., alkanes. The Treszczanowicz-Kehiaian association theory has been applied to the association part of the apparent molar heat capacity, φ_c, of the alcohol in solution, giving ΔH° for H-bond formation and the volume-fraction equilibrium constant K_4^φ for the formation of tetramers. The K_4^φ are related to K_4, an equilibrium constant for H-bond formation in tetramers which is found to be independent of alkanol carbon number from 3 to 16 while it is slightly larger for methanol and ethanol. A common K_4 implies a single corresponding states curve (CSC) of φ_c(assoc) against ψ_1 the number of moles of hydroxyl segments per mole of segments in the solution (essentially molarity) as introduced by Pouchly. Data for 1-alkanol + n-alkane systems follow a CSC characteristic of tetramers rather than CSC predicted by continuous association models, e.g., Mecke-Kempter or Kretschmer-Wiebe. The CSC approach can be applied to enthalpy and residual entropy data. It predicts characteristic concentration dependences of the excess functions; for instance, S^E is positive at low alcohol concentration then negative. The replacement of the inert solvent by a proton-acceptor, e.g., benzene, introduces a new association between the alcohol and the proton-acceptor. Characteristic changes occur in C_p^E and H^E. Grolier and collaborators have found a wide variety of systems for which C_p^E has a surprising W-shape concentration dependence with two minima separated by a maximum, or two regions of positive curvature separated by a region of negative curvature. It is suggested that the W-shape is a consequence of local composition non-randomness caused by large values of H^E and G^E occurring in strongly-interacting systems. C_p^E is the superposition of two contributions. One is negative and of parabolic concentration dependence as found in systems where a component is polar or anisotropic in molecular shape. The other contribution due to non-randomness is positive and large toward the middle of the concentration range, i.e., the critical concentration of the system.

INTRODUCTION

The change of heat capacity on mixing, C_p^E, and the apparent heat capacity, φ_c, of a component are useful thermodynamic tools to study liquid structure in solution. The disadvantage of H^E compared to C_p^E lies in the presence in H^E of a large contribution besides that of structure. This is due to the dispersive force antipathy between the two components, represented by the X_{12} parameter of the Flory theory or the interchange energy of regular solution theory. The temperature dependence of this contribution is slight so that most of C_p^E arises from structure which is usually highly temperature-dependent. Applications have been to correlations of molecular orientations in n-alkane systems (ref. 1), the formation of clathrates or "icebergs" around hydrophobic solutes (ref. 2), the micellization of surfactants (ref. 3) and the formation of micelle-like structures in aqueous mixtures of alcohols and other organic solvents (ref. 4). The present communication will deal with four other situations where structure appears in solution: (1) 1 -alkanols dispersed in an inert solvent, e.g., an n-alkane, where the alcohol molecules cooperatively H-bond into tetramers. (2) 1-alkanols dispersed in an "active" solvent, e.g., CCl_4, benzene, an ether or an ester or (3) dispersed in a binary mixture of an active and an inert solvent. In these systems, the alcohol molecules may either self-associate or complex with the active molecules; (4) systems of extremely high H^E (>1000 J mol^{-1}) and G^E(>800 J mol^{-1}). Here the antipathy between two components leads to non-randomness or concentration fluctuations with a corresponding contribution to the heat capacity of the systems, and the appearance of a characteristic W-shape concentration dependence of C_p^E, negative towards the edges of the concentration range and positive toward the middle.

1-ALKANOLS IN AN INERT SOLVENT

A molar excess quantity X^E compares the apparent molar quantity φ_X in solution with the same quantity in the pure state, i.e.,

$$X^E = x_1(\varphi_X - X^\circ) \tag{1}$$

Here X can be C_p, H, V or the residual (non-combinatorial) S. Trends in X^E are therefore a reflection of trends in φ_X modulated by the introduction of X° and x_1. In the present systems, φ_X of an alcohol contains (1) the internal X, e.g., enthalpy or heat capacity of the alcohol, (2) an associational or chemical contribution, of primary interest to us, and also, (3) φ_X(phys) due to other "physical" interactions between the alcohol and its molecular surroundings. We now consider the φ_X relative to their values in the limit of infinite dilution of the alcohol:

$$\varphi_X^{rel} = \varphi_X - \lim \varphi_X(x_1 \to 0) \tag{2}$$

Clearly φ_X^{rel} will not contain contribution (1) but does retain φ_X(assoc) since all self-association of the alcohol vanishes at infinite dilution. φ_X^{rel} will also contain the difference in φ_X(phys) values between finite concentration and infinite dilution. When X = V, this contribution is large and may dominate the associational contribution (ref. 5); for X=H the difference is smaller but still important (ref. 6) and finally for X=C_p the physical contribution appears to be negligible in the present systems. Thus,

$$\varphi_c^{rel} = \varphi_c(assoc) = \varphi_c - \lim \varphi_c(x_1 \to 0) \tag{3}$$

For H-bonded systems, this sensitivity of C_p to association structure, and its insensitivity to the physical interaction constitutes, we believe, an important advantage. φ_c(assoc) has now been obtained (ref. 7) for seventeen 1-alkanol-n-alkane systems. A variety of curves as a function of concentration are found each with a maximum in φ_c and φ_c(assoc) occurring at different alcohol mole fractions or weight fractions depending on the system. However, a more fundamental concentration variable has been advanced (ref. 8), i.e., a concentration of hydroxyl groups in the solution,

$$\psi_1 = \text{no. OH groups/total groups}$$

$$= x_1/(x_1 r_A + x_2 r_2) \tag{4}$$

with r_A and r_2 being the numbers of segments in the alcohol and the inert solvent, respectively. ψ_1 is related to the molarity M_1 through

$$\psi_1 = M_1 v/1000 \tag{5}$$

where v is the molar volume of the segment taken to be 40.7 $cm^3 mol^{-1}$ the molar volume of methanol. Plotting against ψ_1, φ_c(assoc) for all the alcohol-inert systems now fall on a single curve with the exception of methanol and ethanol systems which deviate slightly. Fig. 1 shows the data for the dilute range, i.e., $x_1 \leq \approx 0.1$.

The steep increase of φ_c(assoc) at very low ψ_1 corresponds to the onset of alcohol self-association, in fact as tetramers, followed by a maximum and a long decrease to the pure alcohol which is not seen in fig. 1. Thus the maximum in φ_c(assoc) and in "structure" does not occur for the pure alcohol where there is the highest degree of H-bond formation, but at a very low concentration, $\psi_1 = 0.004$ or $x_1 \approx 0.01$ where the unassociated hydroxyls would be 26 Å apart. "Structure" implies H-bonding probability weighted by the distance through which the hydroxyls are drawn together in forming the multimers.

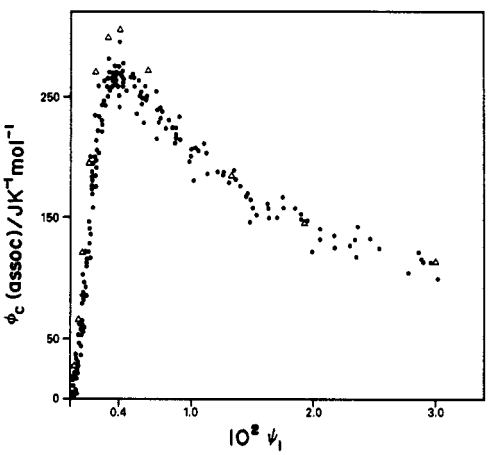

Fig. 1. $\varphi_c(assoc) = \varphi_c^{rel}$ against ψ_1 in the dilute range for seventeen alkanol-n-alkane mixtures. Data for ethanol n-decane (Δ).

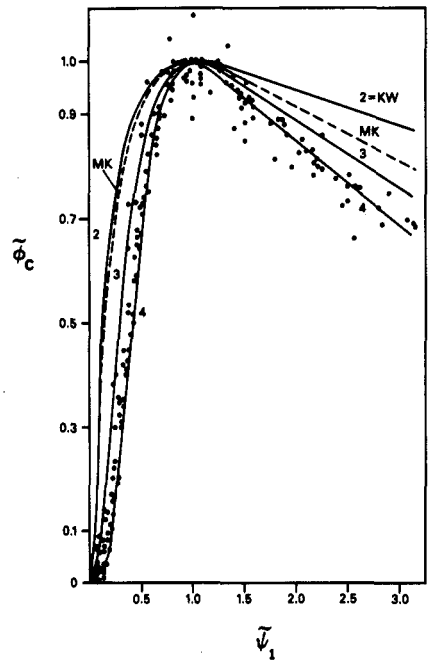

Fig. 2. Reduced $\tilde{\varphi}_c$ against $\tilde{\psi}_1$ in dilute range for systems of fig. 1. Also theoretical curves for dimer, trimer, tetramer, KW and MK models.

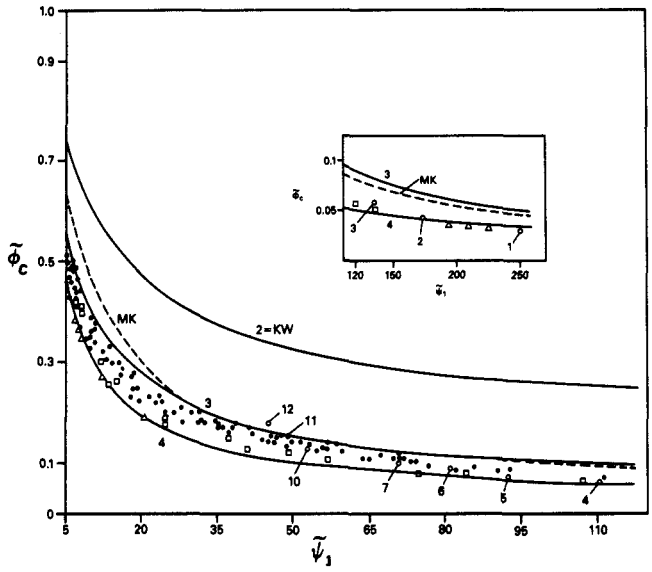

Fig. 3. Reduced $\tilde{\varphi}_c$ against $\tilde{\psi}_1$ at higher alcohol concentration for 21 alkanol-n-alkane systems. Data for pure alkanols (0) indicated by carbon numbers. Also theoretical curves for dimer, trimer, tetramer, KW and MK models.

Association theory can be used to relate φ_c(assoc), to the thermodynamics of alcohol self-association. The Treszczanowicz-Kehiaian (TK) model (ref. 9) uses a H-bonding enthalpy ΔH° and alcohol self-association equilibrium constants K_i^φ for the formation of i-mers:

$$K_i^\varphi = \varphi_{Ai} / (\varphi_A)^i \qquad (6)$$

where φ_{Ai} and φ_A are the volume fractions of, respectively, the alcohol i-mers and monomers. ΔH° and K_i^φ have been fitted (ref. 6,7) to the φ_c(assoc)-x data and indicate the predominance of tetramers, as well as a rapid decrease of K_4^φ with increasing alcohol chain-length. The K_i^φ have been interpreted (ref. 10) through the more fundamental H-bonding constants using the Flory lattice theory (ref. 11). A later version (ref. 12) of this theory gives (ref. 7).

$$(K_i^\varphi)^{1/i-1} V_A = K_i (i)^{i/i-1} \upsilon \sigma w^2 / z \qquad (7)$$

Here K_i is the H-bonding equilibrium constant for formation of the i-mer, V_A is the alcohol molar volume, σ the i-mer symmetry number, w an i-mer flexibility parameter and z the lattice co-ordination number. $K_i = \exp(-\Delta H_i^\circ/RT)\exp(\Delta S_i^\circ/R)$ with ΔH_i° and ΔS_i° the enthalpy and entropy of H-bond formation in the i-mer. The K_i should be independent of the alcohol whose chain-length is taken into account by V_A but the K_i^φ are different, for different i-mers. If the K_i^φ are replaced by the more fundamental K_i, then the TK theory predicts that φ_c(assoc) should be a universal function of ψ_1, i.e., a corresponding states curve (CSC) as found experimentally in fig. 1. A particularly simple case arises if the solution contains predominantly multimers of a single type, e.g., i = 4, as is found experimentally. Then, the co-ordinates of the maximum of the CSC are

$$\frac{\varphi_c(\text{assoc. max})}{R[(i-1)\Delta H^\circ/RT]^2} = \frac{1}{i(i^{1/2}+1)^2} \qquad (8)$$

$$\frac{\psi_1(\text{max})}{(K_i \sigma w^2/z)^{-1}} = \frac{1+i^{-1/2}}{i^{3/[2(i-1)]}}$$

For cyclic i-mers the factor $(i-1)\Delta H^\circ$ is replaced by $i\,\Delta H^\circ$. The co-ordinates of the maximum in fig. 1 are φ_c(assoc. max) = 270 ±12 J K^{-1} mol^{-1} and ψ_1(max) = 4.0 ±0.4 x 10^{-3} which with i=4 give ΔH° = -28.3 ±0.6 kJ mol^{-1} and ΔS_4° = -46.6 ±JK^{-1} mol^{-1} for the formation of the H-bonds in linear tetramers. For cyclic tetramers each value is multiplied by 3/4. One should notice in fig. 1 that φ_c(assoc. max) and ψ_1(max) are different for ethanol and probably methanol. For the former φ_c(assoc. max) = 305 J K^{-1} mol^{-1} and ψ_1(assoc. max) = 3.4 x 10^{-3}.

The co-ordinates of the maximum may be used as scaling or reduction parameters for the CSC to give a reduced $\tilde{\varphi}_c$-$\tilde{\psi}_1$ curve where

$$\tilde{\varphi}_c = \varphi_c(\text{assoc})/\varphi_c(\text{assoc. max})$$
$$\tilde{\psi}_1 = \psi_1/\psi_1(\text{max}) \qquad (9)$$

The reduced curves depend only on the value of i chosen, e.g., 2,3, or 4 and are independent of ΔH_i, K_i, etc. and whether the i-mers are cyclic or linear. They are also independent of T which enters only through the scaling parameters. Thus, the same reduced CSC should be obtained not only for data from any 1-alkanol + inert solvent system, but for data at different temperatures.
The applicability at different T has not been tested but fig. 2 and 3 show the reduced CSC from the 25° data of fig. 1 together with data at higher concentration all scaled with experimental values of φ_c(assoc. max) and ψ_1(max).

Figs. 2 and 3 also show reduced CSC given by the TK model for i=2, 3 and 4 and also for the Kretschmer-Wiebe (KW) and Mecke-Kempter (MK) continuous association models (ref. 7) where the K_i are assumed to be the same for all i-mers, the former model being based on the Flory-Huggins combinatorial entropy and the latter on the ideal entropy. It is a curious fact that the KW reduced curve is identical to the curve for dimers, the only difference between the two cases being in the values of the scaling parameters, i.e., ΔH° and K. Fig. 2 indicates that in the dilute range only the i=4 model is satisfactory, a conclusion also arrived at by fitting the TK model to heat capacity data in unreduced form. The slow increase of φ_c(assoc) with ψ_1 seen in fig. 2 followed by a sharp upturn corresponds to the plateau of H^E/x_1 found by Stokes and collaborators (ref. 13). This was followed by a steep decrease of H^E/x_1 with increasing concentration. These ΔH results first showed the inadequacy of the KW and MK models in the dilute range and the requirement of considering a predominance of higher multimers, i.e., pentamers in ref. 14. At higher concentration fig. 3 shows that there is a deviation of the data toward the i=3 curve but as discussed in ref. 7 it is difficult to believe that the multimer size actually decreases from tetramers. The favouring of tetramers by the alcohols from methanol to hexadecanol indicates that self-association is a co-operative process similar to (reverse) micellization. Furthermore, it suggests that the tetramers are cyclic rather than linear since the tetramer is the first cyclic multimer to form without drastic distortion of the H-bonds. Blander and Curtiss (ref. 15) have studied the self-association of methanol and ethanol and other associated molecules in the vapour phase through thermal conductivity measurements. Tetramers are again found to be predominant and the cyclic form is confirmed by quantum mechanical calculations (ref 16).

The CSC approach may be extended to the enthalpy and entropy of alcohols in inert solvents (ref. 17). Fig. 4 shows a plot against ψ_1 of φ_H^{rel} relative to φ_H at infinite dilution as given by

$$\varphi_H^{rel} = H^E/x_1 - \lim(H^E/x_1)(x_1 \to 0) \qquad (10)$$

The experimental data from ref. 13 for ethanol, + cyclohexane, + n-heptane and + n-hexadecane all fall on essentially the same CSC which is also obeyed by data at concentrations higher than those shown in fig. 4. Other data for n-propanol, n-hexanol and n-decanol in n-alkanes are available (ref. 18) and these also fall on the same CSC. This, however, is surprising since from the φ_c measurements ethanol constitutes a special case. Pending confirmation of values of $\lim H^E/x_1(x_1 \to 0)$ for these alcohols we only consider the ethanol data. The figure also shows curves of the associational φ_H^{rel} calculated with different models fitted to the φ_c results. First, the fit was made to $\varphi_c(\text{max}) = 270\ \text{J K}^{-1}\ \text{mol}^{-1}$ and $\psi_1(\text{max}) = 4 \times 10^{-3}$ which are valid for the majority of the alkanols. The curves come from the following models: tetramers, dimers, KW and MK, although the last is not seen in fig. 4 since it is almost identical to KW. In fig. 4 the dimer, KW and MK models are clearly incorrect. As pointed out first by Stokes and collaborators, higher multimers are needed. Nevertheless, the MK model has been successfully used at higher concentrations in dealing with H^E (ref. 6). Only the tetramer curve in fig. 4 is in qualitative agreement with the data. It displays the slow decrease of φ_H^{rel} at low ψ_1 followed by a sharp drop characteristic of cooperative self-association. Fig. 4 shows another tetramer curve specially calculated for ethanol using constants fitted to φ_c(assoc. max) and ψ_1(max.). This new curve passes through the data points within experimental error, which is at first sight, surprising because it seems to imply that there is no physical contribution present. In a simple Flory-Huggins treatment we have

$$\varphi_H^{rel}(\text{phys}) = - zW_H\psi_1 \qquad (11)$$

with W_H the interchange energy for the OH -CH_2 contact taken independent of the alkanol. At the low values of ψ_1 in fig. 4 the physical contribution to φ_H^{rel} is too small to be seen, but at higher values of $\psi_1 \simeq 0.1 - 0.5$ the experimental CSC does lie below the associational curve and the difference may be interpreted as ψ_H^{rel}(phys) which is slightly different for the ethanol-alkane and ethanol-cyclohexane systems.

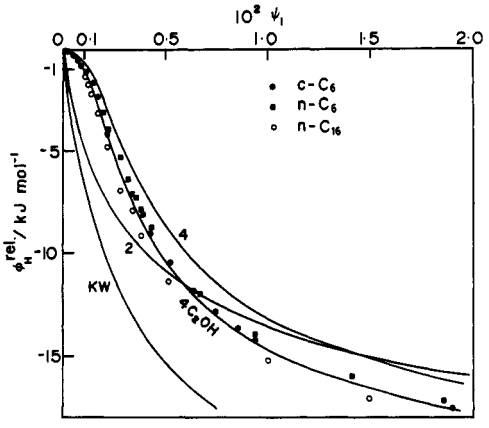

Fig. 4. Alcohol enthalpy in solution, φ_H^{rel}, against hydroxyl concentration, ψ_1, in dilute range. Ethanol-hydrocarbon data from ref. 13. Also theoretical curves valid for majority of alcohols using dimer, tetramer and KW models and for ethanol systems using tetramer model.

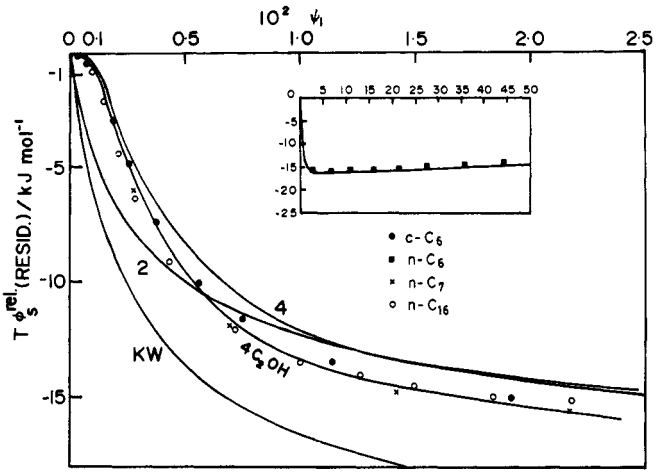

Fig. 5. Alcohol residual entropy in solution, $T\varphi_s^{rel}$(resid.) against hydroxyl concentration ψ_1 in dilute range. Ethanol-hydrocarbon data from ref. 13 and H.C. Van Ness, C.A. Soczek and N.K. Kochar, J. Chem. Eng. Data, 12, 346 (1967) and V.C. Smith and R.L. Robinson, ibid, 15 (1970). Theoretical curves identified as in fig. 4.

It is of interest that the slopes of φ_H^{rel}(assoc) and φ_H^{rel}(phys) against ψ_1 are both negative, both in fig. 4 and at higher concentrations. Thus using eq. (1) both H^E(assoc) and H^E(phys) are positive throughout the concentration range and at all T. This contrasts with S^E which is negative through most of the concentration range.

Fig. 5 shows the corresponding residual or non-combinatorial part of the relative apparent molar entropy $T\varphi_s^{rel}$ of ethanol in cyclohexane, n-hexane and n-hexadecane. This quantity was obtained using activity coefficient data from ref. 13, subtracting off the Flory-Huggins combinatorial free energy and making use of φ_H^{rel}. The data are seen to follow a CSC which at low ψ_1 looks like φ_H^{rel}. The figure also gives $T\varphi_S^{rel}$ curves calculated with the same parameters used with φ_H^{rel}. The tetramers curve calculated with parameters valid for most of the alcohols is in qualitative agreement with the data, while the dimers, KW and MK do not respect the cooperative character of the experimental curve. (MK curve omitted since it is so similar to the KW). Again the special tetramers curve for ethanol is in remarkable agreement with the data. The accord at higher ψ_1 is shown in the insert. Again using the Flory-Huggins lattice theory we have

$$\varphi_S^{rel}(\text{phys}) = -zW_S\psi_1 \qquad (12)$$

where W_S is the physical interchange entropy for the OH-CH_2 contact, expected to be positive. However, the agreement between the predicted associational $T\varphi_S^{rel}$ and the experimental curve is within the experimental error, particularly in the parameters used in our calculation. It is therefore difficult to say if there is any physical contribution to $T\varphi_S^{rel}$ at all.

The qualitative aspects of $T\varphi_s^{rel}$ curve are interesting. The negative values of course indicate the non-randomness introduced into the solution through tetramer formation. The slope of $T\varphi_s^{rel}$ against ψ_1 is first negative and then for higher concentration it becomes positive (fig. 5, insert) whereas the slope for φ_H^{rel} continued negative, this feature being seen experimentally and for all theoretical models. Thus, in spite of continuously increasing H-bonding as ψ_1 increases, a minimum in the residual entropy occurs at low ψ_1 after which the residual entropy increases. This behaviour arises from non-randomness or "structure" reflecting the distance through which the alcohol molecules are drawn together to form the multimers. The residual entropy of alcohol molecules in the pure state is higher than in the solution at all but the most dilute concentrations. Thus according to eq. (1) TS^E(residual) is positive at low concentration and negative through the remainder of the concentration range. The Flory-Huggins combinatorial contribution to TS^E is positive but can hardly eliminate the negative sign when added to TS^E(residual) to give the total. Thus the S-shape TS^E concentration dependence is expected to be general for all alcohols and all T. Finally, the same approach described here for H and S may be applied to φ_V^{rel}(A.J. Treszczanowicz, unpublished).

1-ALKANOLS + A PROTON ACCEPTOR

Fig. 6 shows H^E, C_p^E and φ_c for ethanol mixed with the inert solvent hexane (I) and also with benzene, of similar molar volume to hexane. Benzene is a proton acceptor (PA) with which the ethanol can H-bond as well as self-associating into tetramers. In the fig. H^E (PA) < H^E(I) at extremely low x but is considerably larger throughout most of the concentration range. It is surprising that the introduction of the PA increases H^E even though it interacts favourably with the alcohol. For C_p^E and φ_c three concentration regions are visible. For both these thermodynamic functions, (1), at very low x<0.01, PA>I; (2), for higher x≈0.1, PA<I; and finally, (3), x>0.2, PA>I. These qualitative effects of a PA on the thermodynamic functions seem to hold generally unless the alcohol-PA interaction is stronger than the alcohol-alcohol interaction and unless there is a large difference in molecular size of the two components. The present article also compares φ_c for hexanol + n-C_{12} and + methyl acetate in fig. 9. In apparent contradiction to the above there is no region (3) where C_p^E, φ_c are larger for the PA system. However, the molar volume of n-C_{12} is considerably larger than that of MA and this increases φ_c and C_p^E of the former system causing the region 3 to disappear.

These effects of changing an inert to a PA solvent can be understood through the alcohol energy, φ_H, shown in fig. 7 as a function of temperature. The fig. is schematic but based on TK calculations fitted to φ_c for the ethanol-benzene system using a variation of eq. 1 in ref. 20. Three energy levels are seen corresponding to self-associated tetramers (A_4) at $3/4\Delta H^\circ$ = -21,290 J mol^{-1}, the alcohol-PA complex (AB) at -13,900 J mol^{-1} fitted to the ethanol-benzene system, and finally complete dissociation of the alcohol at 0 J mol^{-1}. Curves 1,2,and 3 give the temperature variation of the alcohol energy φ_H, at the above-mentioned concentrations 1,2, and 3 in an inert solvent (dotted) and in the PA solvent (full). Curve • represents the pure alcohol. For every curve, at low enough T, the alcohol is part of a self-associated tetramer and hence lies at the lowest energy level. With increasing T, φ_H rises and ultimately reaches the top level, i.e., 0. At any T the slope $d\varphi_H/dt$ of the curve against T gives φ_c. In the inert case the A_4 break up to give monomers directly, while in the PA case they first give AB complexes which then dissociate to give monomers. In both cases the temperature at which the A_4 break up increases with alcohol concentration, i.e., from curve 1 to curve 3 and then the curve for the pure alcohol. However, the temperature in the PA case is lower than in the inert case since the AB level is lower than the monomer level and hence is more easily attained. In contrast to the tetramers, the AB complexes only contain a single alcohol molecule and hence dissociate at a concentration-independent temperature which in our case lies below T' the experimental temperature. The curves for the PA case seen in the fig. correspond to a resultant of the $A_4 \rightarrow$AB and AB dissociations.

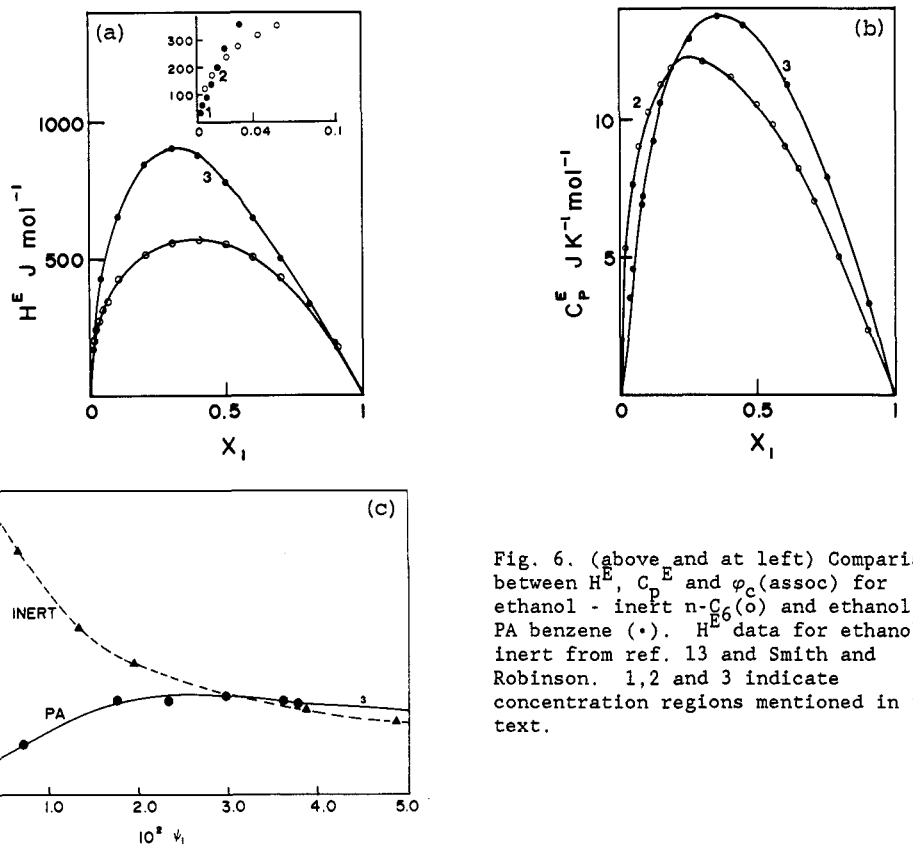

Fig. 6. (above and at left) Comparison between H^E, C_p^E and φ_c(assoc) for ethanol - inert n-C_6(o) and ethanol - PA benzene (•). H^E data for ethanol - inert from ref. 13 and Smith and Robinson. 1,2 and 3 indicate concentration regions mentioned in the text.

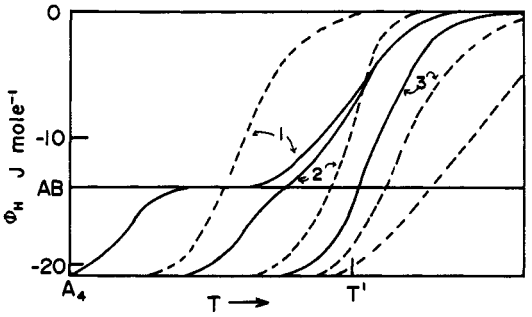

Fig. 7. (at left) Schematic of energy φ_H of alkanol in inert solvent (dotted curves) and proton acceptor (full curves). Energy levels correspond to tetramers A_4, alcohol-PA complex AB and dissociation 0. Increasing concentration 1,2 and 3 and pure alcohol •. T' corresponds to experimental temperature.

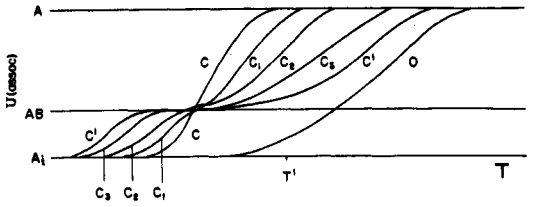

Fig. 8. Schematic of energy φ_H of alcohol at the same low concentration in the following inert solvent (C), increasing concentration of PA in PA - inert mixture (C_1, C_2 and C_3), the pure PA (C') and pure alcohol.

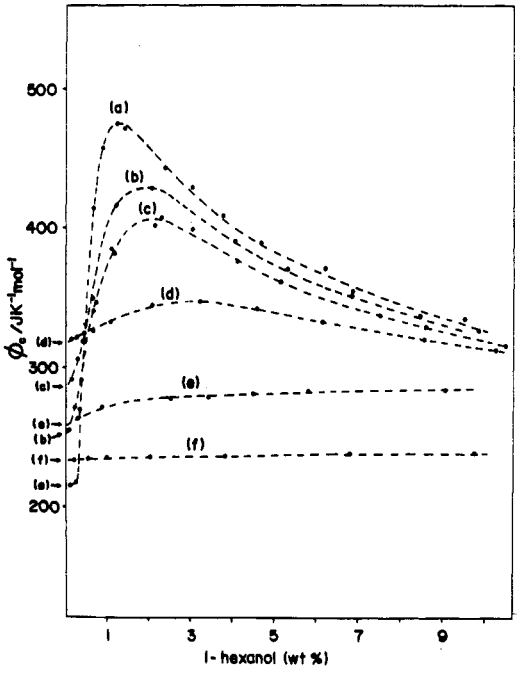

Fig. 9. φ_c of hexanol as a function of its concentration in (a) n-dodecane, (f) methyl acetate(MA) and in MA-dodecane mixtures having the following MA wt %: b, 2.0; c. 4.3, d, 10.2; e, 30.0.

The different dissociations take place at different T. For the lowest concentration, (1), the A_4 dissociate in the PA at the lowest temperature, then the A_4 dissociate in the inert solvent, and finally the AB dissociation lies at the highest temperature. Thus at T' the alcohol in the inert is almost dissociated, i.e., φ_H and φ_c are at the 0 level. However, in the PA case the alcohol is still freeing itself from the AB complex and φ_H is still negative and φ_c positive. According to eq. (1). H^E and C_p^E are found through subtracting H^o and C^o_p from φ_H and φ_c. H^o is close to the lowest level and $C_p{}^o$ is small. Thus H^E is + for both inert and PA cases but $H^E(I)>H^E(PA)$. The slope $\varphi_c(PA)$ and $C_p^E(PA)$ are larger than $\varphi_c(I)$ and $C_p^E(I)$ as in the figure.

At the higher concentration (2), the temperature of dissociation in the inert has caught up with the temperature of AB dissociation which has hardly changed. Then in the fig. $\varphi_H(PA)\approx\varphi_H(I)$ and the HE values are equal for the inert and PA systems. However, the slope against T of the inert curve is larger than in the PA case and hence $\varphi_c(PA)<\varphi_c(I)$ as seen in fig. Finally at conc. (3), the dissociation temperature of A_4 in the inert is now at the highest temperature, higher than the full line resultant of the $A_4 \rightarrow AB$ and AB dissociations which has been "held back" by the AB dissociation. In neither the inert nor the PA case is the alcohol substantially dissociated, but dissociation is even less for the inert than the PA case, and hence $H^E(PA)>H^E(I)$. Correspondingly, $d\varphi^H/dT$ and also φ_c and c_p^E are larger for the PA system.

In this qualitative treatment H^E(phys) has been ignored since the main trends are determined by the association contribution. It seems to us that alcohol-PA thermodynamics is a fruitful area in which simple models can lead to a satisfying qualitative picture.

ALCOHOL + PROTON ACCEPTOR + INERT SOLVENT SYSTEMS

An alcohol dispersed in a proton acceptor-inert solvent mixture is capable of the same three energy levels as in fig. 7. They are seen again in fig. 8 where the curves represent an alcohol in its pure state, o, and at the same very low alcohol concentration in an inert solvent (C), in binary mixtures of the inert with increasing amounts of a proton-acceptor, (C_1, C_2,C_3) and in the pure proton-acceptor (C'). As the concentration of PA is increased the AB level is increasingly attractive to the alcohol, so that the φ_H(assoc) curves above the AB energy level are displaced towards higher temperature and below the AB level towards lower T. Fig. 8 is helpful in understanding the experimental φ_c(assoc) curves for the 1-hexanol + methyl acetate + n-dodecane mixtures shown in fig. 9. Substitution of an inert hydrocarbon solvent by a proton-acceptor + hydrocarbon mixture produces drastic changes in the concentration dependence of φ_c(assoc). In fig. 8 at the experimental temperature T' and at constant very low alcohol concentration increasing PA concentration causes the slope $d\varphi_H/dT$ to rise from its value in the inert (curve C) to a maximum (curve C_2) and then drop to the value in the proton acceptor solvent (curve C'). This corresponds to the experimental behaviour seen in fig. 9 for infinite dilution of the 1-hexanol as the methyl acetate concentration is increased. At higher alcohol concentration, as the concentration of methyl acetate is increased φ_c(assoc) drops continuously from the alcohol + inert to the alcohol + PA curve. This behaviour is also understandable from a higher concentration version of fig. 8.
In fig. 9 the experimental φ_c(assoc) is compared with the TK calculations. Parameters of the theory were fitted to the alcohol + inert φ_c(assoc) curve and to the infinite dilution value for φ_c(assoc) in the binary alcohol + proton acceptor. The curves in fig. 9 for the ternaries and the alcohol + proton acceptor system are thus predictions and not the result of a fitting procedure. Qualitatively, the drop in φ_c(assoc) on increasing methyl acetate concentration corresponds to a lowering of the degree of alcohol structure in solution through replacing self-associated multimers by AB complexes. The latter bring together the associating A and B species over shorter distances compared with the association of A monomers at low alcohol concentration, and hence correspond to greater non-randomness and structure.

SOLUTION NON-RANDOMNESS IN HIGHLY NON-IDEAL MIXTURES

Grolier and collaborators (ref. 21) have found a wide variety of systems for which the concentration dependence of the excess heat capacity has a "W-shape", i.e., two minima occur, separated by a maximum or two regions of positive $C_p^E(x)$ curvature separated by a region of negative curvature. Both types of W-shape C_p^E curves are schematically represented in fig. 10. Components 1 and 2 of the systems always differ greatly in chemical nature: compound 1 can be a linear or cyclic ether, ester, nitrile, ketone or chloroalkane while component 2 is a normal, branched or cyclic alkane. A common characteristic of these systems is that they have large H^E>1200 J mol^{-1} and G^E>800 J mol^{-1} values and often are close to phase separation. Recently (ref. 22) it has been proposed that the W-shape C_p^E concentration dependence is due to a deviation of local from bulk composition, i.e., non-randomness in the solution. Here the structure is due to the antipathy between unlike molecules forcing like molecules to "associate".

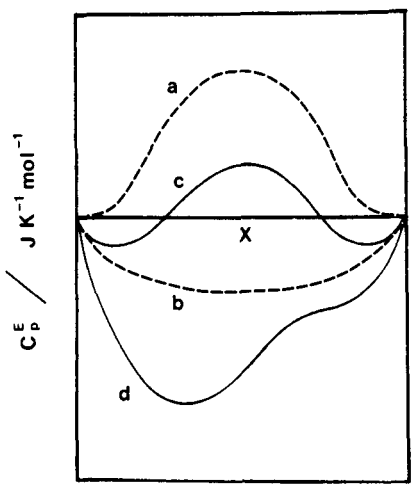

Fig. 10. Schematic C_p^E curves: a, non-randomness and b, random contribution; c, d: total W-shapes.

The W-shape arises then from two C_p^E contributions depicted in fig. 10: a random contribution which is negative and of parabolic concentration dependence and a non-random contribution which, as shown qualitatively by the Guggenheim quasi-chemical theory (ref. 22) is positive, concave downwards in the middle of the concentration range, but concave upwards at the extremes. The non-randomness contribution falls to zero at both ends of the concentration range in accordance with the intuitive requirement that when either component is dispersed at high dilution in the other, it must tend to be randomly distributed. As a result, the non-random C_p^E contribution has the correct concentration dependence to give the W-shape when added to the random contribution.

A more direct measurement of non-randomness is given (ref. 23) by the concentration-concentration correlation function S_{cc} which is related to the inequality of distribution of component 1 molecules around a component 2 molecule or a component 1 molecule, i.e., non-randomness. S_{cc} is given by

$$S_{cc} = \left(\frac{\partial^2 G/RT}{\partial x^2}\right)^{-1}_{P,T} = \frac{x_2 RT}{(\partial \mu_1/\partial x_1)_{P,T}} \qquad (13)$$

where μ_1 is the chemical potential of component 1. Hence, S_{cc} reflects the concentration fluctuations and is attainable through light scattering measurements. Using the Flory-Huggins (FH) expression for G^E, eqn (13) becomes

$$S_{cc} = \frac{x_1 x_2}{1 + \frac{x_1 x_2 (r-1)^2}{(x_1 + r x_2)^2} - \frac{2\chi_1 x_1 x_2 r^2}{(x_1 + r x_2)^3}} \qquad (14)$$

where $r=v_2/v_1$ and $\chi_1 = z\Delta w/KT$ with Δw being the interchange free energy per mole of segments normalized to size of the component 1 molecule and z the lattice coordination number. According to eqn (14) S_{cc} and non-randomness increase with decrease of temperature. It also indicates that molecular size has different effects depending on the size of r. For small values of χ_1, the first term in eqn (14) dominates and S_{cc} decreases as V_2 and r increases. If χ_1 is large, the second term in the denominator of eqn (14) dominates and the maximum in S_{cc} occurs at high concentration of the smaller component. If V_2 and r are increased S_{cc} increases and the maximum moves to higher x_1. The correlation between non-randomness in solution, as measured by S_{cc}, and the appearance of W-shape C_p^E curves is illustrated in fig. 11 where S_{cc} and C_p^E are shown for hexafluorobenzene (HFB) mixed with several alkanes. S_{cc} for HFB+br-C_8 is small and skewed slightly to high HFB concentration whereas for HFB + cC_6 S_{cc} is larger and skewed to lower HFB concentration. Also in fig. 11 calculated S_{cc} values using eqn (14) are displayed; here, χ_1 values were fitted so that theoretical S_{cc} has the same maximum value as the experimental, although not necessarily occurring at the same concentration. This gives χ_1=0.61 and 1.27 for brC_8 and cC_6 respectively. Theoretical S_{cc} values using eqn (14) are seen to give the correct skewing of the curves. For the small S_{cc} mixture, i.e., HFB+brC_8, C_p^E curves are of normal shape both at 25 and 10°C; the negative C_p^E and positive dC_p^E/dT values are consistent with the presence of order in pure HFB and its destruction upon mixing. For HFB+cC_6, although S_{cc} is now larger than for HFB+brC_8, C_p^E still does not have a W-shape; it is less negative, however, and on decreasing the temperature to 10°C the W-shape becomes evident. This change in C_p^E shape is clearly due to increasing non-randomness, i.e., increasing S_{cc}.

Fig. 11 also shows C_p^E for HFB + dicyclohexyl and +brC_{16}. Here, components 2 are of similar chemical character to cC_6 and brC_8 but are of greater molecular size. Comparing HFB + cC_6 and dicyclohexyl, it is clear that the effect of increasing molecular size of component 2 is to enhance the W-shape character and to move the maximum from low cyclic concentration to

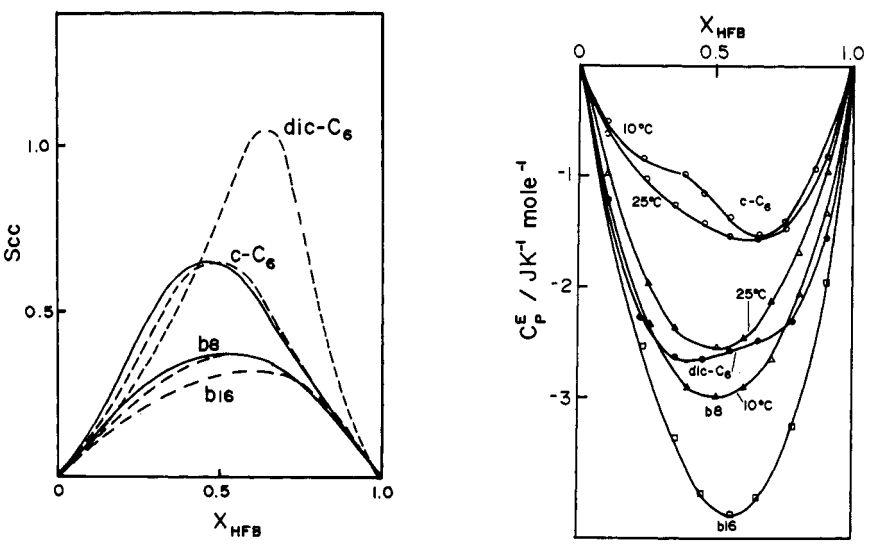

Fig. 11. S_{cc} and C_p^E curves for hexafluorobenzene (HFB) mixed with 2,2,4-trimethylpentane (b8), cyclohexane (c-C_6), 2,2,4,4,6,8,8-heptamethylnonane (b 16) and dicyclohexyl (di-C_6). Dashed curves in S_{cc} are calculated.

high. On the other hand, comparing HFB + brC_8 and + brC_{16}, the effect of increasing molecular size is the opposite: C_p^E shows no W-shape for brC_{16} and is in fact more negative than for brC_8. These effects are explained by non-randomness and S_{cc} given by eqn (14), where the χ_1 values for dicyclohexyl and brC_{16} may be taken equal to the values found for cC_6 and brC_8 respectively. Fig. 11 shows that in going from cC_6 to dicyclohexyl, the increase of r has made the second term in eqn (14) dominant increasing S_{cc} and displaying it to higher HFB concentration. Clearly, this increase and displacement of S_{cc} corresponds to the behaviour of C_p^E. For HFB + brC_{16} and + brC_8 (low χ_1 value) the first term in eqn (14) dominates and then S_{cc} decreases as r is increased from brC_8 to brC_{16}. Correspondingly, C_p^E is more negative for brC_{16} and there is no W-shape concentration dependence.

Acknowledgements

Financial support of the Natural Science and Engineering Research Council of Canada and the Ministère de l'Education du Québec is gratefully acknowledged. We thank the Journal of the Chemical Society, Faraday Transactions 1 for permission to reprint figs. 1-3.

REFERENCES

1. S.N. Bhattacharyya, M. Costas, D. Patterson and H.V. Tra, Fluid Phase Equilbria, 20, 27 (1985).
2. S.J. Gill, S.F. Dec, G. Olofson and I. Wadso, J. Phys. Chem., 89, 3758 (1985).
   A. Hvidt, Ann. Rev. Biophys. Biolog., 12, 1 (1983).
3. J.E. Desnoyers, Pure Appl. Chem., 54, 1469 (1982); A.H. Roux, D. Hetu, G. Perron and J.E. Desnoyers, J. Soln. Chem., 13, 1 (1984).
4. G. Roux, G. Perron and J. Desnoyers, J. Soln. Chem., 7, 639(1978).
5. A.J. Treszczanowicz and G.C. Benson, Fluid Plane Equilibria, 41, 31 (1988).
   A. Heintz, Ber. Bunsenges. Phys. Chem., 89, 172(1985).
6. A. J. Treszczanowicz and M. Rogalski, Bull Acad. Pol. Chim., 34, 143 (1986).
7. L. Andreoli-Ball, D. Patterson, M. Costas and M. Caceres, J.C.S. Faraday 1, in press.
   M. Costas and D. Patterson, J.C.S. Faraday 1, 81, 635 (1985).
8. J. Pouchly, J.C.S. Faraday 1, 82, 1609 (1986).
9. H. Kehiaian and A.J. Treszczanowicz, Bull. Acad. Chim. France, 5, 1561 (1969).
10. (a) H. Renon and J.M. Prausnitz, Chem. Eng. Sci., 22 299 (1967); Errata, ibid, 22, 1891 (1967); (b) V. Brandani, Fluid Phase Equil.
11. P.J. Flory, J. Chem. Phys., 12, 425 (1944).
12. P.J. Flory., Proc Royal Soc. A, A234, 60 (1956).
13. R.H. Stokes and C. Burfitt, J. Chem. Thermodyn. 5, 623 (1973).
    R.H. Stokes and M. Adamson, J. Chem. Thermodyn. 8, 683 (1976).
    R.H. Stokes and M. Adamson, J.C.S. Faraday 1, 73, 1232 (1977); H.T. French, A. Richards and R.H. Stokes, J. Chem. Thermodyn., 11, 671 (1979).
14. R.H. Stokes, J. Chem. Soc Faraday Trans 1, 73, 1140 (1977).
15. (a) L.A. Curtiss, D.J. Frurip and M. Blander, J. Phys. Chem., 86, 1120 (1982); (b) D.J. Frurip, L.A. Curtiss and M. Blander, Int. J. Thermophys., 2, 115 (1981).
16. L.A. Curtiss, J. Chem. Phys., 67, 1144 (1977).
17. P. Paquet and D. Patterson, to be published.
18. M.K. Woycicka and W.M. Recko, Bull. Acad. Pol. Chim., 20, 783 (1972).
19. M.K. Woycicka and B. Kalinowska, Bull. Acad. Pol. Chim., 23, 759, 1975).
20. M. Costas and D. Patterson, J.C.S. Faraday 1, 81, 655 (1985).
21. M. Pintos, R. Bravo Baluja, M.I. Paz Andrade, G. Roux-Desgranges and J.P.E. Grolier, Can. J. Chem., 66, 1179 (1988) and refs. therein.
22. M.E. St. Victor and D. Patterson, Fluid Phase Equilibria, 35, 237(1987).
23. R.G. Rubio, M. Caceres, R.M. Masegosa, L. Andreoli-Ball, M. Costas and D. Patterson, to be published.